Synthesis of Nano-Ag Doped Acrylic Acid/Acrylamide Composites: Synergistic Effects on Biological and Antimicrobial Activity

Gufran Ali Mohamad[1], Mustafa Katan Shneshil[1], Ali Jaffar Saleem[1] and Mohammed Bouskout[2]
[1]*Department of Chemistry, College of Education for Pure Sciences, University of Diyala, 32001 Baqubah, Iraq*
[2]*Laboratory of Microbial Biotechnologies, Agrosciences and Environment (BioMAgE), Labeled Research Unit-CNRSTN°4, Cadi Ayyad University, 40000 Marrakesh, Morocco*
pch.ghofranali@udiyala.edu.iq, Mustafa.Shneshil@udiyala.edu.eq, alijaffar3@yahoo.com, mohammed.bouskout@ced.uca.ma

Keywords: 1,3,4-Thiadiazole; Hydrogel; Acrylic Acid; Acrylamide; Nanocomposites; Nano Silver; Antibacterial Activity.

Abstract: The increasing prevalence of antibiotic-resistant bacterial pathogens has created an urgent need for developing new antimicrobial materials with improved efficacy and safety. In this study, novel thiadiazole-based poly(acrylic acid-co-acrylamide) hydrogels incorporated with silver nanoparticles (AgNPs) were synthesized and investigated as potential antibacterial agents. A series of 2-amino-5-substituted-1,3,4-thiadiazole derivatives containing ortho-chloro, meta-chloro, phenyl, and para-nitro groups were prepared and introduced into acrylic acid/acrylamide hydrogel networks through emulsion polymerization. The prepared hydrogel composites were characterized using X-ray diffraction (XRD), scanning electron microscopy (SEM), and thermogravimetric analysis (TGA) to evaluate their structural, morphological, and thermal properties. The antibacterial activity of the synthesized composites was examined against multidrug-resistant clinical isolates of Staphylococcus aureus and Klebsiella pneumoniae using agar well diffusion and minimum inhibitory concentration (MIC) assays. The results demonstrated that the AgNP-loaded hydrogel composites exhibited significant antibacterial activity, with the effectiveness depending on the chemical structure of the thiadiazole substituent. The meta-chloro, phenyl, and para-nitro derivatives showed strong inhibitory effects against S. aureus, whereas the ortho-chloro derivative exhibited the highest activity against K. pneumoniae. The MIC results revealed that the ortho-chloro composite achieved the strongest activity against K. pneumoniae with an MIC value of 16 µg/mL, while the meta-chloro composite showed improved activity against S. aureus with an MIC value of 32 µg/mL. Cytotoxicity assessment indicated good compatibility at concentrations up to 64 µg/mL, with toxicity increasing at higher concentrations. These findings suggest that thiadiazole-functionalized AgNP hydrogel composites are promising candidates for future antimicrobial and biomedical applications.

1 INTRODUCTION

Bioactive materials and specially ones with antibacterial activity are drawing a lot of attention from medical community [1]. These may consist of a wide range of material types, using metallic elements, polymeric structures and antibacterial agents [2]. Due to their excellent properties, Hydrogel are among the most widely used biomaterials in modern medical and scientific fields, with applications ranging from contact lenses and drug carriers to medical implants, tissue engineering, integrated cancer diagnostics and treatment [3]. Furthermore, the removal of heavy metallic ions [4], supercapacitors [5]. In this context, hydrophilic polymers serve as the foundation for preparing hydrogels, which are materials known for their capability to uptake and hold significant volume of water. These materials constitute a significant category, described as hydrophilic Hydrogel networks with the ability to absorb and hold substantial quantities of water or biological fluids, without maintaining their structural stability [6]. Hydrophilic hydrogels are commonly stabilized through covalent (chemical) or non-covalent (physical) bonds that give rise to both the physical and chemical diversity of hydrogels and contain functional groups such as hydroxyl, carboxyl, amide, sulfonic acid, and amine [7], [8]. Hydrogels have become a subject of considerable research, with the greatest challenge remaining the development of

hydrogels possessing excellent mechanical properties, self-adhesion capabilities, and resistance to deformation [9], [10]. Polyacrylic acid-based gels are widely used for these purposes. However, they are often modified with synthetic or natural polymers, and through copolymerization, which means [11]. Polyacrylic Acid Hydrogels may not meet the necessary mechanical strength requirements for practical applications, thus limiting their effectiveness [12]. Therefore, it has become necessary to combine them with monomers such as acrylamide to form networks capable of highly efficient water absorption [13]. Recent studies indicate that incorporating heterocyclic units into polymer structure gives polymers advanced functional properties. Functional polymers contain non-carbon atoms such as N and S within their basic structure, which contributes to improved reactivity and performance in advanced applications [14]. Since macromolecules including enzymes, vitamins, natural products, bioactive compounds, play an important role in these applications, which are important branches of medicinal chemistry [15]. In this context, Thiadiazole systems attract substantial focus due to their diverse spectrum of biological effects, especially antimicrobial activity, as well as their low toxicity, biostable properties, and mesoionic nature, which gives them good cellular permeability and a high reactivity with biomolecules such as proteins and nucleic acids [16], [17]. The 1,3,4-thiadiazole derivatives derive their biological importance from being biosimilars, (Bio isosteres) of pyrimidine bases, giving them the ability to inhibit DNA replication [18]. Their messianic nature also contributes to facilitating cell membrane crossing and improving oral absorption and bioavailability, thus enhancing their binding accuracy to biological targets [19]. Silver nanoparticles (Ag- NPs) have high and broad-spectrum antiviral and antimicrobial properties, even against virulent and drug-resistant strains, and had been defined as an anti-inflammatory agent [20]. Research has also started studying anticancer properties of silver nanoparticles [21], [22]. Depending on the material of carrier silver ions, reactive oxygen species or adsorption of nanoparticles could be the mechanism of antimicrobial action [23]. The efficacy of these strategies has been demonstrated when incorporated into nanofiber technologies. demonstrated the efficacy of silver poly (vinyl alcohol)/zeolite fibers against Klebsiella pneumoniae and Staphylococcus aureus due to their large surface area [24]. Poly acrylamide hydrogels doped with silver nanoparticles [25]. Antibacterial activity of a silver nanocomposite of palm resin and poly acrylamide were investigate for their antibacterial activity [26]. Tea Polyphenol–Poly (acrylic acid) Hydrogels doped with silver nanoparticles were served as Cytotoxicity materials [27].

2 EXPERIMENTAL PROCEDURES

2.1 Materials and Chemicals

Acrylic acid, 98% ($C_3H_4O_2$) (AA), acrylamide (C_3H_5NO, 99%), sodium dodecyl sulfate (SDS, $C_{12}H_{25}SO_4Na$, 97%), (2-chloro, 3- chloro ,4- nitro) benzoic acid (C_6H_4–R–COOH), phosphorus oxychloride ($POCl_3$, 99%), thiosimcarbazide (CH_5N_3S, 98%), potassium persulfate (KPS,$K_2S_2O_8$, 98%), sodium hydroxide (NaOH, 45%), hydrochloric acid (HCl, 37%), Potassium Hydroxide (KOH,99.9%), dimethyl sulfoxide (DMSO, 97%), tetrahydrofuran (THF, 99%), methanol (CH_3OH, 99.9%), Silver nitrate ($AgNO_3$,100 %), Sodium borohydride ($NaBH_4$,100 %).

2.1.1 Materials for Biological Activity

Staphylococcus aureus and Klebsiella pneumoniae were used as test bacteria. The culture medium use includes blood agar, Mueller-Hinton agar, and broth made from brains and hearts. For bacterial density standardization Biomereriex and McFarland 0.5 solutions were used. They experimented with multiple polymers and nanocomposites. Components of the chemical mixture consisted of 0.01%w/v Rezasurin, Triton X-100 (0.1%), and sodium chloride (0.9%), which was isotonic saline. It consisted of a centrifuge, incubator (35–37 °C), spectrophotometer (540 nm), sterile Petri dishes, swabs, cork drills, 96-well microplates, and a steam sterilizer (121 °C, 15 psi).

2.1.2 Instrument

The recording of infrared spectra of hydrogels and compounds (A1-A4) with a range of frequencies between 400-4000 cm^{-1} was accomplished by KBr disc method with a SHIMADZU IR Affinity spectrometer. ^{1}H-NMR studies of compounds (A1–A4) were recorded on a Burker Ultra Shield spectrometer with a 500 MHz magnet in DMSO-d6 using TMS as a reference. The absorbance of chemicals (A1-A4) and the recorded hydrogels was measurements in the SHIMADZU-1700 dual-band UV–Vi spectrometer, with a quartz cell and KOH as the solvent. Hydrogels were analyzed

thermogravimetrically with a Rheometric Scientific TGA-1000. The hydrogels produced (silver) were characterized spectroscopically using a Zeiss (FESEM): TESCAN, MIRA3, China scanning electron microscope. XRD was performed using a Cu-Ka spectrometer Philips instrument PW 1730 X-ray spectrometer, Netherlands. The settings used to operate this instrument were: 30kV, 20 mA, and 80 ° — 20 ° = 10 °. XRD study was performed using CuKα radiation λ = 0.15406 nm.

2.1.3 Synthesis of 1,3,4-Thiadiazole Compounds

10 mL of $POCl_3$ was dissolved in 100mL flask and then added 0.01 mol of substituted benzoic acid and 0.01 mol of thiosemicarbazide. The mixture was heated for three hours before adding 30 mL of distilled water, after which the reaction was heated for a further four hours. A total of 10% of the mixture was added to neutralize at a pH of 6. Then we filtered the solution to obtain the chemicals we needed filtered, washed the precipitation several times by distilled water and dried [28].

- 2-amino-5-(2-chlorophenyl)-1,3,4-thiadiazole (A1). Yellowish crystalline powder, yield (80%), m.p 213-215°C, Rf = 0.39; F.T-IR (KBr disk, cm^{-1}) 3283-3136, 3071, 1624, 1593, 1427.
- 2-Amino-5-(3- chlorophenyl)-1,3,4-thiadiazole (A2). Pale yellow powder, yield (81%), m.p 215-217 °C, Rf = 0.40; F.T-IR (KBr disk, cm^{-1}) 3290-3125, 3063, 1624, 1574,1458.
- 2-Amino-5-(phenyl)-1,3,4-thiadiazole (A3). Light powder, yield (95%), m.p 224-226°C, Rf = 0.33; F.T-IR (KBr disk, cm^{-1}) 3275-3086, 3062, 1631, 1581, 1442.
- 2-Amino-5-(4-nitrophenyl)-1,3,4-thiadiazole (A4). Yellow powder, yield (95%), m.p. 257–261 °C, Rf = 0.52; F.T-IR (KBr disk, cm^{-1}) 3360–3300, 3090, 1637, 1595, 1520,1345.

2.1.4 Synthesis of Hydrogels (oCIT-g-AAcAm, mCIT-g-AAcAm, PT-g-AAcAm, pNT-g-AAcAm)

Synthesis of hydrogels that were prepared using emulsion polymerization. Substituted 1,3,4-thiadiazole derivatives (0.5 g) were first dissolved in acrylic acid (5 mL) with continuous stirring, gently heating where necessary. Acrylamide (5 g) was then added to system to the previous mixture. were dissolved under stirring and with mild heating when necessary. After dissolving all components, 20 mL of a 0.01 g/mL sodium dodecyl sulfate (SDS) was added, and then 20 mL of distilled water. Stir continuously until an emulsification of homogenous texture is obtained. The reaction mixture (H_2O) was then heated to 70 °C, potassium persulfate (KPS) (0.02 mol) was added to the mixture as the initiator. After polymerization was complete, the resulting polymer was isolated and repeatedly washed with distilled water and methanol to yield the final hydrogel.

- oCIT-g-AAcAm: color Pale yellow, F.T-IR (KBr, νmax, cm^{-1}) 3650-2925(O-H), 3448-3360(NH_2), 3086 (CH_{aromat}),2916-2870(C-H_{alfa}),1716(C=O), 1624(C=N),1545 (C=C), ^{1}H-NMR (DMSO-d^6:δ 10.7ppm (1H, COOH), δ 7.2-7.6 (Ar–H), δ (6.4) ppm (2H,NH_2) δ 2.6(H, CH),2.5-3 (2H, CH_2 of polymer chain).
- mClT-g-AAcAm: color white, F.T-IR (KBr, νmax, cm^{-1}) 3642-2865 (O-H), 3423-3393 (NH_2), 3122 (CH_{aromat}),2992-2875 (C-H_{alfa}),1735 (C=O), 1655 (C=N),1553 (C=C), ^{1}H-NMR(DMSO-d^6 :δ 10.7 ppm (1H, COOH), δ 7.2 -7.6 (Ar–H), δ (6.4) ppm (2H,NH_2) δ 3.1 (H, CH),2.5 (2H, CH_2 of polymer chain).
- PT-g-AAcAm: color Pale yellow, F.T-IR (KBr, νmax, cm^{-1}) 3645-2890(O-H), 3455-3356(NH_2),3072 (CH_{aromat}),2954-2870 (C-H_{alfa}),1714 (C=O), 1618 (C=N),1541(C=C), ^{1}H-NMR(DMSO-d^6 :δ 10.5 ppm (1H, COOH), δ 7.9-8.4 (Ar–H), δ (4.4) ppm (2H,NH_2) δ2.7 (H, CH),1.8 (2H, CH_2 of polymer chain).
- pNT-g-AAcAm): color brown, F.T-IR (KBr, νmax, cm^{-1}) 3633-2922 (O-H), 3423-3350, (NH_2), 3095 (CH_{aromat}), 2930-2848 (C-H_{alfa}), 1714(C=O), 1622 (C=N),1547 (C=C), ^{1}H-NMR (DMSO-d^6:δ 10.6ppm (1H, COOH), δ 7.7 -8 (Ar–H), δ (6.3) ppm (2H,NH_2) δ4.4 (H, CH),1.8 (2H, CH_2 of polymer chain).

2.1.5 Solubility of Hydrogels

The prepared hydrogels were dissolved in 0.1 g portions of each hydrogel specimen and added to 20 mL of various solvents, including dimethyl sulfoxide (DMSO), tetrahydrofuran (THF), N, N-dimethylformamide (DMF), water, methanol, 10% w/v potassium hydroxide solution, and 10% w/v hydrochloric acid solution. The samples were immersed in the solvents 24 hours at room temperature, after which their solubility was evaluated by visual inspection. The results were recorded as dissolved or insoluble.

2.1.6 Swelling of hydrogels

10 mL of distilled water and methanol were carefully added to dry hydrogel (0.1 g). The swelling property was studied through the change in weight of hydrogel

at 0, 6, 9, 12 and 24 h. After each step, samples were removed from the liquid medium, dried on filter paper (to remove excess liquid) and weighed to provide the mass of the swollen hydrogel (Ws). The swelling percentage of the hydrogels was determined according to the following equation:

$$\text{Swelling Percentage (\%)} = \frac{W_s - W_d}{W_d} \times 100.$$

Where: Ws: Weight of the hydrogel after swelling, Wd: Dry weight of the hydrogel.

2.1.7 Synthesis of Silver Nanoparticles

Silver nanoparticles were synthesized using a chemical reduction method. 2 g of silver nitrate ($AgNO_3$) were dissolved in 25 mL of deionized water by continuously stirring in a 100 mL beaker. In another beaker, 1 g of sodium hydroxide (NaOH) was weighed, dissolved in 25 mL of deionized water, and then transferred to a burette. The silver nitrate solution was slowly poured into the sodium hydroxide solution at a stirring temperature of 70 °C, continued until the solution became dark brown which indicates agglomeration of silver nuclei silver. After the addition, the solution was sonicated for 10 min to achieve better homogeneity. Followed by the addition of 0.472 g of sodium borohydride ($NaBH_4$) (molecular weight = 37.83 g/mol), to ensure that reduction was complete, to the solution whilst stirring at 70 °C for 2 h. The precipitate was filtered using the corresponding filter paper for the product, then dried and crushed. The precipitated product was then dried, and the dried product was calcined in an oven to obtain silver nanoparticles (600 °C for 3 hours).

2.1.8 Synthesis of the Polymer Nano-Ag Composites

1 g silver nanoparticles were added to solutions of 1 g of each hydrogel to 1000 ml of water containing 1000 ppm of the produced polymers and 1000 ppm of the silver solution. To obtain a homogeneous composite, the solution was exposed to ultrasonic waves for 1hr, as depicted in scheme 1.

2.3 Antimicrobial Activity

2.3.1 Screening of the biological activity of hydrogels

Two types of clinical isolates were used and were identified using the VITEK 2 system. This is considered a preliminary screening. Staphylococcus aureus and Klebsiella pneumoniae isolates were cultured on blood agar. The bacterial suspension density was standardized using the McFarland 0.5 standard for turbidity. BioMérieux precipitating solution producing approximately 1.5×10^8 cells/ml. Preparation of Muller-Hinton agar 38 g of Muller Hinton medium was added to 1 L of distilled water and sterilized in an autoclave at 121 degrees Celsius 15 pressure points for 15 minutes.

The agar was then autoclaved and poured into sterile Petri dishes before use. The antibacterial activity of the polymers was evaluated using agar well diffusion. The bacteria were transferred to Brain Heart Infusion broth and incubated at 37°C for 18–24 hours. The bacterial suspension was then adjusted according to the McFarland criteria. The bacterial solution was spread in Muller-Hinton agar plates using a sterile brush and the wells were made in the medium using a sterile cork drill. To each well, 100 µL of testing material at different concentrations (100, 50, 25) µg/mL previously conditioned, was added. Antibacterial activities were determined by measuring the widths of the inhibition zones formed around the wells, these were incubated overnight.

2.3.2 MIC Determination by Microplate - (MTP)

The MICs of the experimental compounds were studied in microtiter plates (96 wells) using the sequential dilution method in liquid medium. A standard bacterial suspension (approximately 5×10^5 CFU/mL) was added to each well, and the compounds were diluted in Mueller-Hinton broth as sequential binary serial dilutions. The suspension was diluted to the final volume of 200 µL and the plates were incubated at 35–37 °C for 18–24 hours followed by treating each well with 0.01% w/v resazurin solution and further incubation for an additional 1-3 hours. Subsequently, the minimum inhibitory concentration of the compound was defined as the lowest concentration where the color of the test sample (inside the well) in respect to the positive control sample was not changed after incubation stayed blue instead of pink.

2.3.3 Assay for Hemolytic Toxicology based on Fragility of Red Blood Cells

The solubility of the nanocomposites was assessed using the red blood cell fragility test, following the method described by Dodge et al. (1963) with minor modifications. Fresh human red blood cells were rinsed three times with isotonic solution saline (sodium chloride,0.9%) and resuspended to a

hematocrit of 2 Equal volumes of the red blood cell suspension and composite solutions were combined and incubated at 37 °C for 1 hour. After centrifugation at 1500 rpm for 10 minutes, Complete hemolysis (positive control) was determined using 0.1% Triton X-100, and isotonic saline was used as the negative control. The contents of the hemoglobin in the supernatants were measured at 540 nm by photometric analysis. 100% was then defined as the amount of hemolysis absorbed from erythrocytes lysed in distilled water. Then the percent hemolysis was calculated using the formula:

$$Haemolysis(\%): \frac{\mathrm{Abs}_{\mathrm{sample}}}{\mathrm{Abs}_{\mathrm{erythrocytes\ in\ water}}} \times 100$$

Where A represents the absorption measured at 540 nm. 0-9% non-toxic, 10-49 % slightly toxic, 50-89% toxic, 90-100% highly toxic.

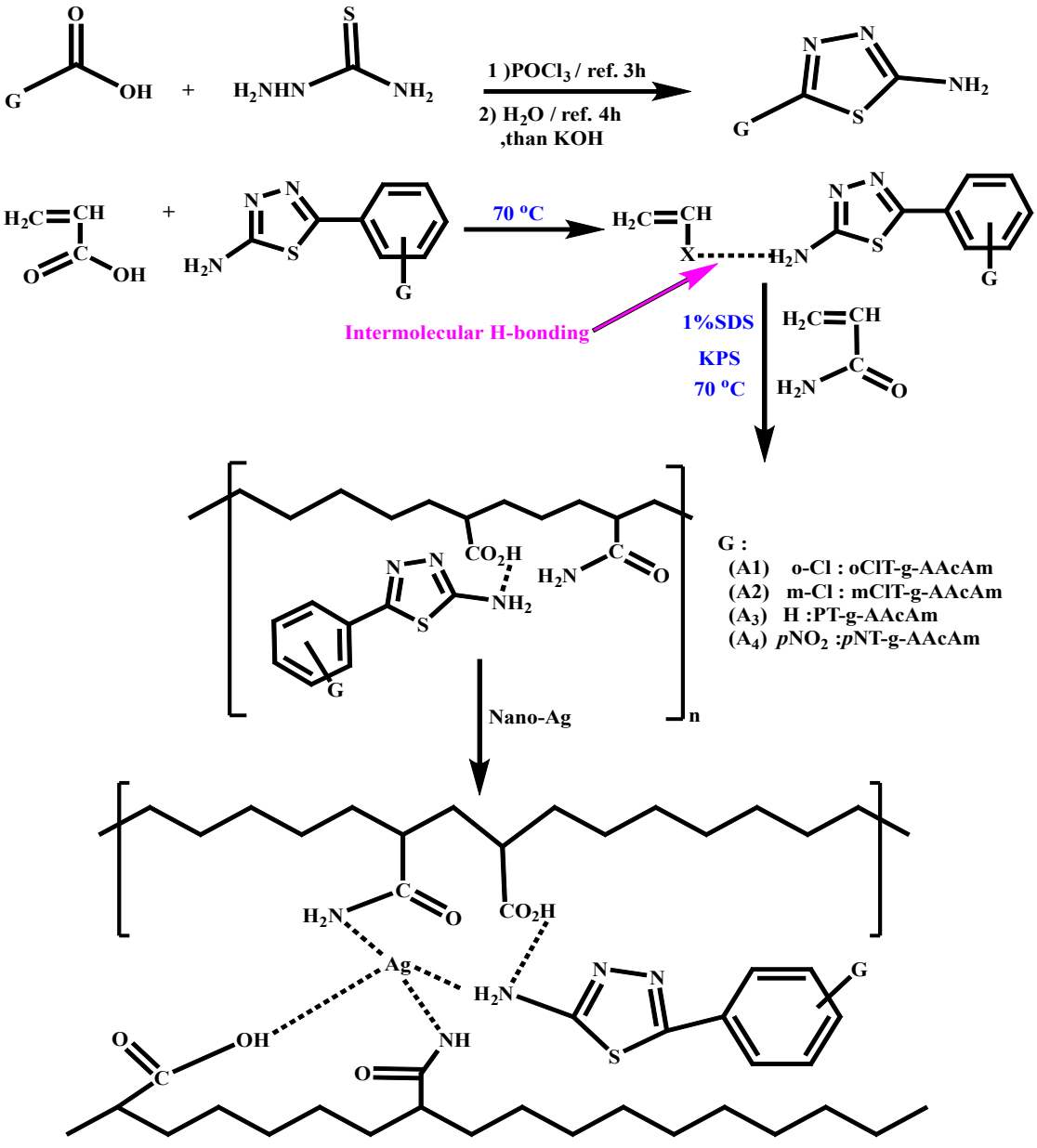

Figure 1: Schematic illustration of nano-Ag composites production with respect to the hydrogel.

3 RESULTS AND DISCUSSION

3.1 2-Amino-5-Substituted Phenyl-1,3,4- thiadiazole (A1-A4)

The hydrogels were obtained from a mixture of thiosemicarbazide and the correct carboxylic acid that was refluxed (A1-A4) with $POCl_3$. Acrylamide was dissolved in a mixture of derivatives (A1-A4) that were previously dissolved in acrylic acid. The net mixture was polymerized by the addition of KPS as an initiator using emulsion polymerization (oClT-g-AAcAm, mClT-g-AAcAm**,** PT-g-AAcAm**,** pNT-g-AAcAm**.** New composites were prepared by mixing the polymers with a nano silver (oClT-g-AAcAm-nano-Ag, mClT-g-AAcAm-nano-Ag**,** PT-g-AAcAm-nano-Ag**,** pNT-g-AAcAm-nano-Ag respectively. The composites were tested as antimicrobial for two antibiotics resistant classified bacterial strands (Staphylococcus aureus) and bacteria (Klebsiella pneumoniae). The results showed that the composites high (mClT-g-AAcAm-nano-Ag**,** PT-g-AAcAm-nano-Ag**,** pNT-g-AAcAm-nano-Ag) and moderate (oClT-g-AAcAm-nano-Ag, activity against the bacteria (Staphylococcus aureus), (oClT-g-AAcAm-nano-Ag) was highly active against (Klebsiella pneumoniae).

3.2 Characterization Thermogravimetric Analysis of Hydrogels (TGA)

Thermogravimetric analysis (TGA) was utilized to investigate the thermal properties. The TGA analysis of hydrogel is presented in Figure2. The weight loss from the hydrogel was in three different stages of decomposition. About 15% weight loss occurred in the temperature range of 100–280°C and may be due to loss of water molecules trapped in the gel network. The second important degradation stage for the hydrogels detected in the range of 280–520°C and related to 45% of weight losses were assigned to the decomposition of carbonyl, NH_2, and COOH functional groups. The third stage, which includes thermal treatment in the range of 520–650°C, indicated a quick weight loss of approximately 90% with respect to the original weight and was ascribed mainly to the dehydration of the polymeric network, depolymerization of the copolymer chains, and fragmentation of the hydrogel network into small carbonaceous molecules. Heating in excess of 650°C showed no further loss in weight.

3.3 Characterization of hydrogels by XRD

X-ray diffraction, or XRD, is one of the most important methods to analyze hydrogel in terms of crystallization and phase composition after preparation. Relative crystallinity of the composite hydrogel was determined by XRD after successful synthesis. Diffraction patterns in the range 10–80° were collected with a Siemens D500 X-ray diffractometer equipped with Cu Kα radiation. X-ray diffraction (XRD) pattern provides essential insights into the crystallinity of the hydrogel. Sharp and intense peaks typically denote a high degree of crystallinity, whereas broad halos are indicative of an amorphous structure. As shown in the X-ray results in Figure 3 a-e, no sharp peaks were detected. Instead, the hydrogel exhibited a broad peak at a value between 15° and 22°, confirming the amorphous solid of the prepared hydrogel.

3.4 Swelling of Hydrogels

The swelling rates in water and methanol depended upon the composition and crosslinking density of the hydrogels, demonstrating their potential for bioregulatory functions and controlled drug release (Fig. 4 and 5).

3.5 Study of Silver Nanoparticles is Composed of Hydrogel using a SEM

The scanning electron microscope images reveal that a hydrogel exhibits an irregular porous three-dimensional network structure formed by the cross-linked polymer chains (Fig. 5).

This porous morphology provides suitable sites for the incorporation of nanoparticles. After loading silver nanoparticles, small spherical or spherical particles are observed on the surface of the hydrogel matrix.

3.6 Antimicrobial Activity

3.6.1 Isolation and Diagnosis

The pathogenic bacterial isolates were identified, which were obtained from burn and wound patients hospitalized at Baquba Teaching Hospital, and were diagnosed using the VITEK 2 system. The results showed that first isolate Staphylococcus aureus bacteria are resistant Benzyl penicillin, Oxacillin and second isolate, Klebsiella pneumoniae, was resistant

to the following antibiotics: Ampicillin, Piperacillin/Tazobactam, Cefazolin, Ceftazidime, Ceftriaxone, Cefepime, Imipenem, Ciprofloxacin, Nitrofurantoin, Levofloxacin and Amikacin patterns to various antibiotics, along with limited susceptibility to certain agents, These findings indicate that the bacterial isolated Klebsiella pneumoniae can be classified as multidrug resistance to antibiotics These results are consistent with the study [29].

3.6.2 Detection of the Antimicrobial Activity Hydrogels

The preliminary detection results shown in Table 1 and Figure 4 showed the biological activity where Staphylococcus aureus bacteria showed that the (HG1) hydrogel dissolved in DMSO, the hydrogel showed moderate activity against the bacteria, and the water-soluble hydrogels (HG2), (HG3), and (HG4) showed high inhibitory activity against bacteria at all concentrations (1000, 500, 250 µg/mL). As for the bacteria Klebsiella pneumoniae, the hydrogels (HG1) showed inhibitory activity at all concentrations (1000,500,250 µg/mL), while the other hydrogels did not show any inhibitory activity against the bacteria. HG1: oClT-g-AAcAm-nano-Ag hydrogel, HG2: mClT-g-AAcAm-nano-Ag hydrogel, HG3: PT-g-AAcAm nano-Ag hydrogel, HG4: pNT -g-AAcAm-nano-Ag hydrogel (Fig. 6 and 7).

3.6.3 Minimum Inhibitory Concentration (MIC)

The resistant isolates under study were subjected to the Minimum Inhibitory Concentration (MIC) test for the hydrogel (HG1, HG2, HG3 and HG4) shown in Table 2 shows the MIC values obtained using successive concentrations (1024,512, 256 128, 64, 64, 32 and 16) µg/mL with Mueller-Hinton-Broth medium. The results of (MIC) assay shown in Table 2 revealed a clear difference in antibacterial potency across the prepared polymers. The hydrogel (HG1) exhibited a higher antibacterial effect against Klebsiella pneumoniae, with a minimum inhibitory concentration value of 16 µg/ml, indicating high efficacy in inhibiting the growth of this Gram-negative bacterium. This result suggests possible interaction between the chemical structure of the compound and the bacterial outer membrane, enhancing its penetration and growth-inhibiting effect.

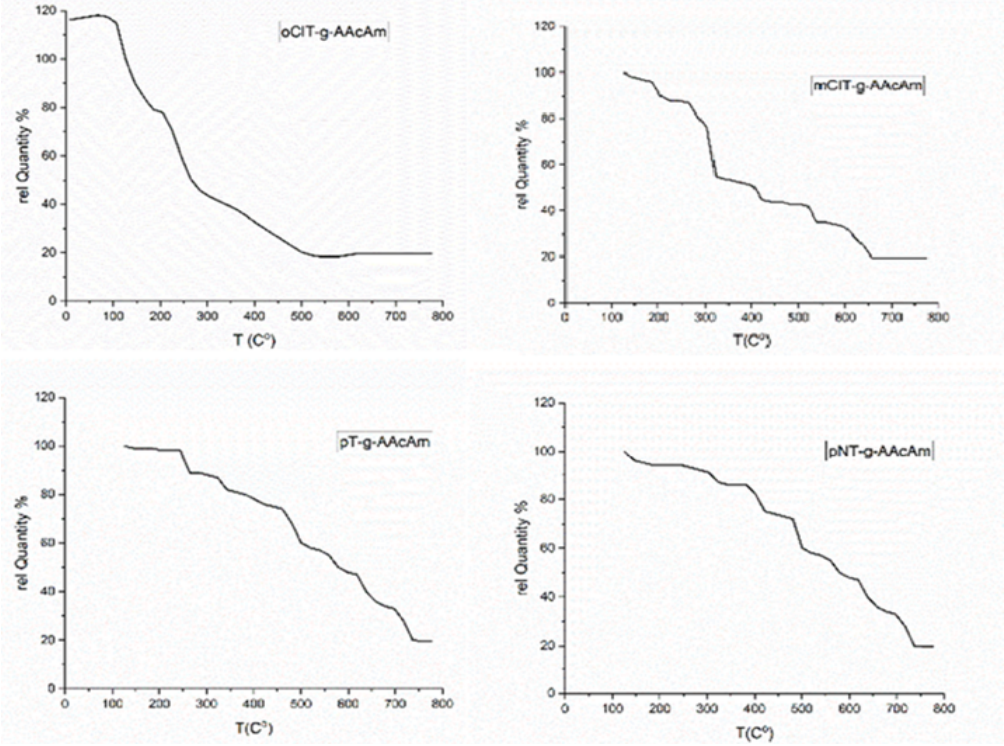

Figure 2: TGA pattern of hydrogel.

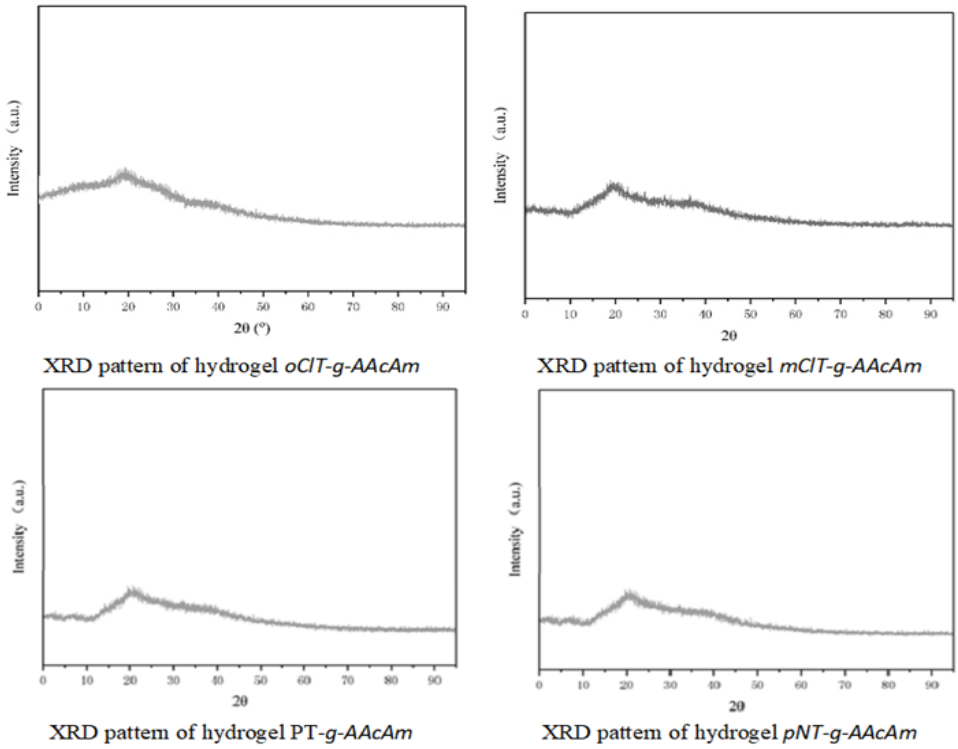

Figure 3: XRD pattern for hydrogel (a) (oClT-g-AAcAm) (b) mClT-g-AAcAm (c) PNT-g-AAcAm (d) pNT-g-AAcAm.

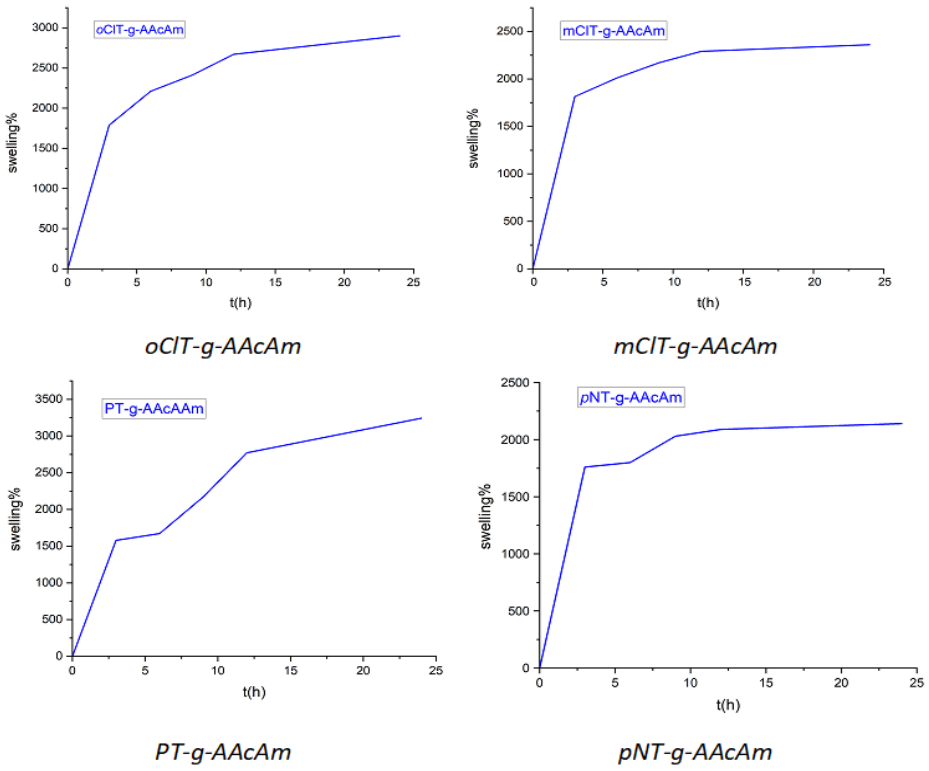

Figure 4: The swelling percentage of hydrogels in water after preparation.

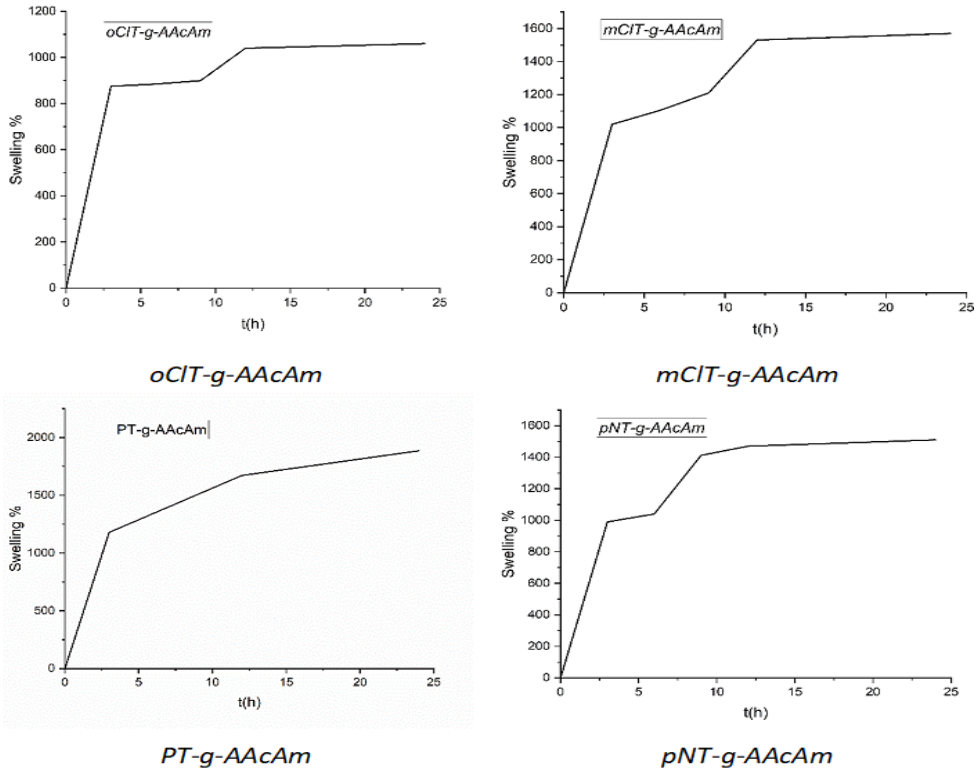

Figure 5: The swelling percentage of hydrogels in Methanol after preparation.

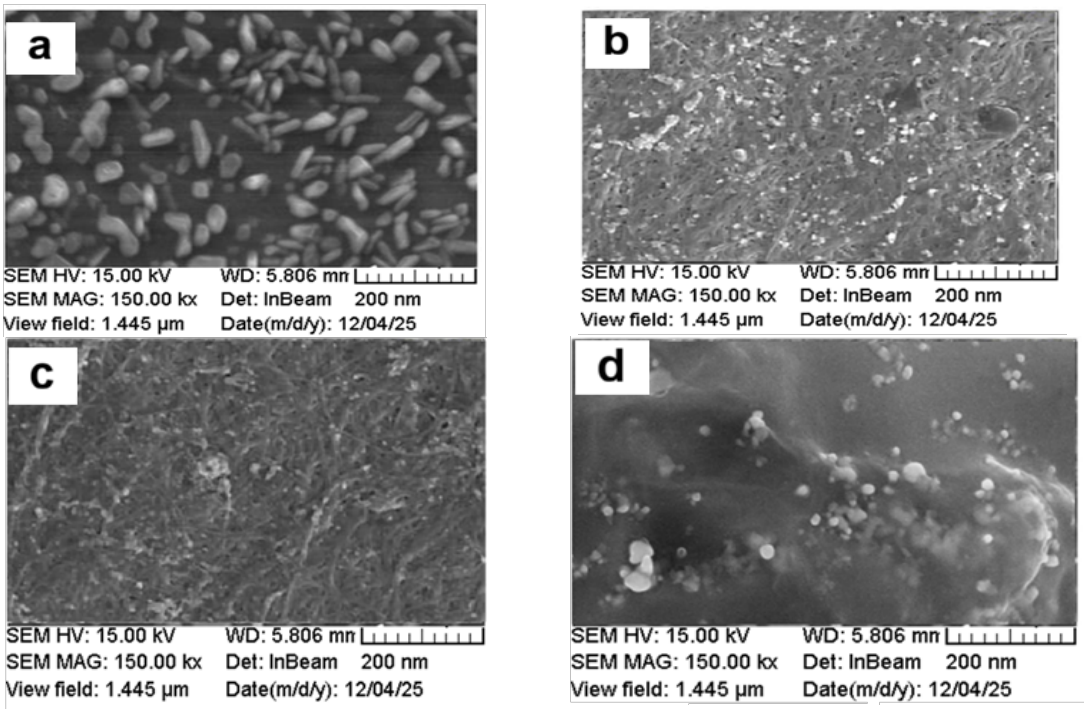

Figure 6: SEM morphology of: a) (oClT-g-AAcAm-nano-Ag), b) (mClT-g-AAcAm-nano-Ag), c) (PT-g-AAcAm-nano-Ag), d) (PNT-g-AAcAm-nano-Ag).

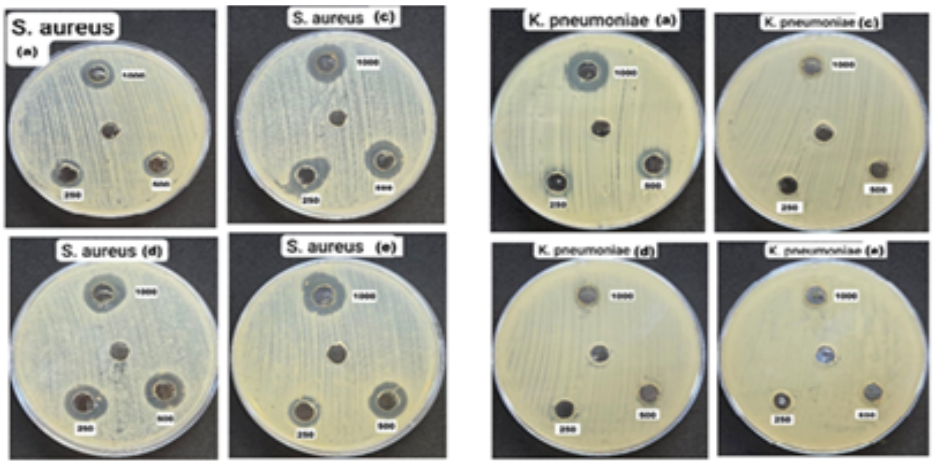

Figure 7: Growth inhibition zones of synthesized graft copolymers/nano-silver particles against S.aureus and K.pneumoniae determined by agar well susceptibility assay (250-1000 µg/mL): a) (oClT-g-AAcAm-nano-Ag), c) (PT-g-AAcAm-nano-Ag), d) (mClT-g-AAcAm-nano-Ag), e) (pNT-g-AAcAm-nano-Ag).

Table 1: Summarizes the preliminary results of polymer screening.

	S. aureus				K. pneumoniae			
Concentration (µg/ml)	100	50	25	C.	100	50	25	C.
oClT-g-AAcAm-nano-Ag (mm)	6	5	5	0	9	5	3	0
mClT-g-AAcAm-nano-Ag (mm)	9	8	6	0	0	0	0	0
PT-g-AAcAm-nano-Ag (mm)	10	8	7	0	0	0	0	0
pNT-g-AAcAm-nano-Ag (mm)	9	7	5	0	0	0	0	0

Regarding the Gram-positive bacterium Staphylococcus aureus, the hydrogel (HG2) showed relatively better activity, with a minimum inhibitory concentration value of 32 µg/ml, compared to the other compounds (HG1, HG3), and (HG4), which registered 64 µg/ml, reflecting moderate antibacterial activity. This difference in efficacy may be ascribed to the structural characteristics of the Gram-positive bacterial cell wall. and the varying permeability of the compounds to or bind with cellular components. Overall, it can be concluded that the hydrogel (HG1) is the most effective among the tested hydrogel, particularly against Gram-negative bacteria, while the hydrogel (HG2) shows promising activity against S. aureus, suggesting an influence of structural composition on biological efficacy.

Table 2: The minimum inhibitory concentration using the ELISA apparatus.

Agent	Bacteria	MIC
oClTg-AAc Am -nano-Ag	K. pneumoniae	16 µg/ml
oClTg-AAc Am-nano-Ag	S. aureus	64 µg/ml
mClT-g-AAc Am-nano-Ag	S. aureus	32 µg/ml
PT- g-AAc Am-nano-Ag	S. aureus	64 µg/ml
pNT- g-AAc Am-nano-Ag	S. aureus	64 µg/ml

3.6.4 Toxicity Test

The cytotoxicity of the (HG1, HG2, HG3 and HG4) were tested at 8, 16, 32, 64, and 128 µg/mL. The test results, shown in Table 3 indicate that the hydrogel were safe (non-toxic) at all concentrations except for 128 µg/mL, which showed a toxic effect through platelet breakdown. All Silver nanoparticle-loaded grafted gels exhibited excellent biocompatibility at low concentrations (8–64 µg/ml). Compared to the positive control (C+), which exhibited complete toxicity (100%), all formulations can be considered safe within this concentration range. Indeed, a significant concentration-dependent toxicity higher toxicity at 128 µg/ml was observed for all the compounds carried out, confirming a dose-dependent biological response. These findings corroborate the described mechanism of action of silver nanoparticles that disturb cytoplasmic membranes, interact with throat (-SH) groups from proteins, cause DNA disruption and generate reactive oxygen species.

Table 3: Results of the compound toxicity test.

No.	Concentration (µg/ml)	Absorbance	Toxicity	Interpretation
oClTg-AAc Am-nano-Ag	8	0.021	1.10%	n
	16	0.019	1.00%	n
	32	0.022	1.16%	n
	64	0.02	1.05%	n
	128	0.648	34.24%	s
mClT-g-AacAm-nano-Ag	8	0.02	1.05%	n
	16	0.014	0.73%	n
	32	0.019	1.00%	n
	64	0.018	0.95%	n
	128	1.572	83.08%	t
PT- g-AAc Am-nano-Ag	8	0.021	1.10%	n
	16	0.042	2.23%	n
	32	0.071	3.75%	n
	64	0.084	4.43%	n
	128	1.749	92.44%	h
pNT- g-AAc Am-nano-Ag	8	0.013	0.68%	n
	16	0.012	0.63%	n
	32	0.022	1.16%	n
	64	0.036	1.90%	n
	128	1.809	95.61%	h
C+		1.892	100%	c
C-		0	0%	n

Note. N: Non-toxic; S: Slighty toxic; T: Toxic; H; Highly toxic.

However, when comparing the different derivatives, the toxicity of hydrogel (HG1), with 34.24% at 128 µg/ml was classified as a low-toxicity compound [30], [31]. These effects combined together cause bacterial cells and biofilms to weaken. This is probably the result of ortho-chlorine substitution, which sterically hinder for direct cell to cell interaction or slower rate of silver ion release. In comparison, HG2 exhibited a high toxicity 83.08% at the same concentration. suggesting that the chlorine group enhances biological interaction by translocating to the meta site. The highest toxicity rates 92·44% and 95·61%, respectively were observed for the HG4 and HG5 derivatives, suggesting that the nature of the substituent group, especially electron-withdrawing group, which plays an important role in biochemical behavior. The end result shows that toxicity at 128 µg/ml is by a synergistic action of silver nanoparticles and thiadiazole units as it contributes to the enhanced reactive oxygen species generation, change in the surface charge and membrane permeability. These results have the same trend with also emphasizing the further importance of substitution patterns of thiadiazole derivatives in the modulating toxic response [32].

4 CONCLUSIONS

In this study, novel thiadiazole-based poly(acrylic acid-co-acrylamide) hydrogel composites loaded with silver nanoparticles were successfully synthesized and evaluated as antimicrobial materials. Structural and thermal characterization confirmed the formation of stable hydrogel networks with porous morphology and predominantly amorphous characteristics suitable for nanoparticle incorporation.

The antibacterial evaluation demonstrated that the synthesized composites exhibited significant activity against multidrug-resistant *Staphylococcus aureus* and *Klebsiella pneumoniae*, with antibacterial performance strongly influenced by the chemical structure of the thiadiazole substituents. The ortho-chloro derivative showed the highest activity against *K. pneumoniae*, while the meta-chloro derivative demonstrated the strongest inhibition of *S. aureus*. The MIC assay confirmed the enhanced antibacterial efficiency of these composites, with values of 16 µg/mL and 32 µg/mL against *K. pneumoniae* and *S. aureus*, respectively.

Cytotoxicity analysis revealed acceptable biocompatibility at effective antibacterial concentrations, while higher concentrations caused concentration-dependent toxicity. Therefore, the incorporation of silver nanoparticles into thiadiazole-functionalized hydrogel networks provides an effective approach for developing new antimicrobial materials. Further investigations, including mechanistic studies and in vivo evaluations, are required to confirm their potential biomedical applications.

REFERENCES

[1] M. A. Huq and S. Akter, "Biosynthesis, Characterization and Antibacterial Application of Novel Silver Nanoparticles Against Drug Resistant Pathogenic Klebsiella pneumoniae and Salmonella enteritidis," Molecules, vol. 26, no. 19, p. 5996, 2021.

[2] M. A. Huq, "Biogenic Silver Nanoparticles Synthesized by Lysinibacillus xylanilyticus MAHUQ-40 to Control Antibiotic-Resistant Human Pathogens Vibrio parahaemolyticus and Salmonella Typhimurium," Frontiers in Bioengineering and Biotechnology, vol. 8, p. 597502, 2020.

[3] S. Suárez-García, R. Solorzano, R. Alibes, F. Busque, F. Novio, and D. Ruiz-Molina, "Antitumour Activity of Coordination Polymer Nanoparticles," Coordination Chemistry Reviews, vol. 441, p. 213977, 2021.

[4] R. Sahraei, Z. S. Pour, and M. Ghaemy, "Novel Magnetic Bio-Sorbent Hydrogel Beads Based on Modified Gum Tragacanth/Graphene Oxide: Removal of Heavy Metals and Dyes from Water," Journal of Cleaner Production, vol. 142, pp. 2973-2984, 2017.

[5] H. Li et al., "Ultrastretchable and Superior Healable Supercapacitors Based on a Double Cross-Linked Hydrogel Electrolyte," Nature Communications, vol. 10, no. 1, p. 536, 2019.

[6] T. Khandaker et al., "Recent Progress in Gel Catalysts: Boosting Efficiency for Sustainable Energy Applications," Catalysis Science & Technology, vol. 15, no. 5, pp. 1357-1389, 2025.

[7] S. N. Nair and S. Sujith, "Hydrogels and Organogels as Food Delivery System," in *Handbook of Nutraceuticals: Science, Technology and Engineering*, Springer, 2026, pp. 849-893.

[8] N. Thang, T. Chien, and D. Cuong, "Polymer-Based Hydrogels Applied in Drug Delivery: An Overview," Gels, vol. 9, p. 523, 2023.

[9] K. Prusty and S. K. Swain, "Nano Silver Decorated Polyacrylamide/Dextran Nanohydrogels Hybrid Composites for Drug Delivery Applications," Materials Science and Engineering: C, vol. 85, pp. 130-141, 2018.

[10] M. Sultan, A. Abdelhakim, and M. Nassar, "Cellulose-Based Hydrogels as Smart, Green and Controllable Nitrogenous Fertilizers Releasing Agents," Journal of Testing and Evaluation, vol. 49, no. 4, pp. 2479-2490, 2021.

[11] A. E. Stoica, C. Chircov, and A. M. Grumezescu, "Hydrogel Dressings for the Treatment of Burn Wounds: An Up-to-Date Overview," Materials, vol. 13, no. 12, p. 2853, 2020.

[12] M. Madaghiele, C. Demitri, A. Sannino, and L. Ambrosio, "Polymeric Hydrogels for Burn Wound Care: Advanced Skin Wound Dressings and Regenerative Templates," Burns & Trauma, vol. 2, no. 4, pp. 2321-3868.143616, 2014.

[13] G. Sennakesavan, M. Mostakhdemin, L. K. Dkhar, A. Seyfoddin, and S. J. Fatihhi, "Acrylic Acid/Acrylamide Based Hydrogels and Its Properties - A Review," Polymer Degradation and Stability, vol. 180, p. 109308, 2020.

[14] E. S. Alsolami, H. S. Alorfi, K. A. Alamry, and M. A. Hussein, "One-Pot Multicomponent Polymerization Towards Heterocyclic Polymers: A Mini Review," RSC Advances, vol. 14, no. 3, pp. 1757-1781, 2024.

[15] A. R. Shaikh, M. Farooqui, R. Satpute, and S. Abed, "Overview on Nitrogen Containing Compounds and Their Assessment Based on 'International Regulatory Standards'," Journal of Drug Delivery and Therapeutics, vol. 8, no. 6-S, pp. 424-428, 2018.

[16] Y. Hu, C.-Y. Li, X.-M. Wang, Y.-H. Yang, and H.-L. Zhu, "1,3,4-Thiadiazole: Synthesis, Reactions, and Applications in Medicinal, Agricultural, and Materials Chemistry," Chemical Reviews, vol. 114, no. 10, pp. 5572-5610, 2014.

[17] D. H. Ibrahim, A. J. Saleem, A. A. Awad, H. S. Ahmed, and M. K. Shneshil, "Antioxidant and Antibacterial Activity of Some 2-Amino-1,3,4-Thiadiazole Schiff's Bases," Journal of Physics: Conference Series, vol. 1294, no. 5, Art. no. 052029, 2019, doi: 10.1088/1742-6596/1294/5/052029.

[18] S. Janowska, A. Paneth, and M. Wujec, "Cytotoxic Properties of 1,3,4-Thiadiazole Derivatives - A Review," Molecules, vol. 25, no. 18, p. 4309, 2020.

[19] D. Kumar et al., "Mechanism-Based Approaches of 1,3,4-Thiadiazole Scaffolds as Potent Enzyme Inhibitors for Cytotoxicity and Antiviral Activity," Medicine in Drug Discovery, vol. 17, p. 100150, 2023.

[20] L. Z. Flores-López, H. Espinoza-Gómez, and R. Somanathan, "Silver Nanoparticles: Electron Transfer, Reactive Oxygen Species, Oxidative Stress, Beneficial and Toxicological Effects. Mini Review," Journal of Applied Toxicology, vol. 39, no. 1, pp. 16-26, 2019.

[21] A. Baran et al., "Ecofriendly/Rapid Synthesis of Silver Nanoparticles Using Extract of Waste Parts of Artichoke (Cynara scolymus L.) and Evaluation of Their Cytotoxic and Antibacterial Activities," Journal of Nanomaterials, vol. 2021, no. 1, p. 2270472, 2021.

[22] Baran et al., "Ecofriendly Synthesis of Silver Nanoparticles Using Ananas comosus Fruit Peels: Anticancer and Antimicrobial Activities," Bioinorganic Chemistry and Applications, vol. 2021, no. 1, p. 2058149, 2021.

[23] Carvalho et al., "Silver Oxide Coatings Deposited on Leathers to Prevent Diabetic Foot Infections," Surface and Coatings Technology, vol. 442, p. 128338, 2022.

[24] H. G. Kim and J. H. Kim, "Preparation and Properties of Antibacterial Poly(Vinyl Alcohol) Nanofibers by Nanoparticles," Fibers and Polymers, vol. 12, no. 5, pp. 602-609, 2011.

[25] Ferrag et al., "Polyacrylamide Hydrogels Doped with Different Shapes of Silver Nanoparticles: Antibacterial and Mechanical Properties," Colloids and Surfaces B: Biointerfaces, vol. 197, p. 111397, 2021.

[26] S. Subash Chandrabose, V. Jaisankar, A. Parameswari, and M. Leo Edward, "Development of Novel Palm Resin-Poly(Acrylamide) Based Hydrogel Silver Nanocomposite for Antibacterial Activity," Iranian Journal of Chemistry and Chemical Engineering, vol. 43, no. 2, 2024.

[27] Y. Liao, C. Xiang, and F. He, "AgNPs@Tea Polyphenol-Poly(Acrylic Acid) Hydrogel Dressing with Synergistic Antibacterial Action and Low Cytotoxicity," ACS Applied Bio Materials, vol. 8, no. 6, pp. 5129-5137, 2025.

[28] M. K. Al-Malki, A. S. Hameed, and A. H. Al-Dujaili, "Synthesis and Mesomorphic Properties of New Columnar Liquid Crystal Containing 1,3,5-Triiminebenzene with Pendant 1,3,4-Thiadiazole Group," Molecular Crystals and Liquid Crystals, vol. 593, no. 1, pp. 34-42, 2014.

[29] M. R. Al-Aajem, H. M. Jasim, and A. J. Saleem, "Detection of Virulent Genes Khe, iuc, rmp, magA in Klebsiella pneumoniae Isolated from Urinary Tract Infection," International Journal of Drug Delivery Technology, vol. 11, no. 4, pp. 1470-1473, 2021.

[30] M. R. F. Muslim, L. Chabib, B. E. Suryaningsih, F. Hayati, and V. Annisa, "Green-Synthesized Silver Nanoparticle Hydrogels for Biofilm-Infected Wounds: Bridging Sustainability and Clinical Translation," Frontiers in Pharmacology, vol. 16, p. 1694144, 2025.

[31] S. H. Rashid and A. Saleem, "Molecular Investigation of the mqsA and mqsR Genes in the Multidrug-Resistant Bacterium Klebsiella pneumoniae," Microbes and Infectious Diseases, vol. 7, no. 2, pp. 1243-1253, 2026.

[32] Y. Zhao, Z. Dai, H. Huang, J. Tian, and H. Cai, "Injectable Silver Nanoparticle-Based Hydrogel Dressings with Rapid Shape Adaptability and Antimicrobial Activity," Applied Biochemistry and Biotechnology, vol. 197, no. 2, pp. 821-836, 2025.